X-ORCA - A Biologically Inspired Low-Cost Localization System

Enrico Heinrich[1], Marian Lüder[1], Ralf Joost[1], and Ralf Salomon[1]

University of Rostock, 18051 Rostock, Germany,
{enrico.heinrich,marian.lueder,ralf.joost,ralf.salomon}@uni-rostock.de

Abstract. In nature, localization is a very fundamental task for which natural evolution has come up with many powerful solutions. In technical applications, however, localization is still quite a challenge, since most ready-to-use systems are not satisfactory in terms of costs, resolution, and effective range. This paper proposes a new localization system that is largely inspired by auditory system of the barn owl. A first prototype has been implemented on a low-cost field-programmable gate array and is able to determine the time difference of two 300 MHz signals with a resolution of about 0.02 ns, even though the device is clocked as slow as 85 MHz. X-ORCA is able to achieve this performance by adopting some of the core properties of the biological role model. hardware implementation, robotics, architecture

1 Introduction

Localization is a process in which some reference points, angles, and distances are used in order to determine the coordinates of new, so-far unknown points. For this task, nature provide several quite powerful solutions. One particularly interesting solution is provided by the auditory system of the barn owl [7]. This solution propagates the sensory information along some neural pathways across the owl's brain. Since the two "wires" are anti-parallel, the attached phase (or correlation) detectors all observe different time delays between the two acoustic signals that originate from the owl's ears.

Section 2 proposes a technical model, called X-ORCA, that mainly adopts some of the main properties of the biological role model. Conceptually, the correlation neurons are modeled by phase detectors. Each phase detector consists of a simple XOR gate and a counter. The counter value represents the average fireing rate of the modeled neuron, and is displayed as a simple number. Internally, the system employs these phase detectors are placed along two anti-parallel "delay wired". Since these wires go along opposite directions, all the phase detectors observed different signal phases as the barn owl's auditory system does as well.

In the domain of electrical engineering, electromagnetic signals are often prefered over acoustic ones, since they travel very large distances with high reliability and low energy consumption. However, electromagnetic signals travel with the speed of light $c \approx 3 \cdot 10^8$ m/s, which makes them quite challenging for every *digital* system, if it comes to high resolutions: a difference in length of

$\Delta x = 1\,\text{cm}$, for example, corresponds to a time difference of $\Delta t \approx 33\,\text{ps}$. Because the X-ORCA system is intended to detect signal delays in the range of a few pico seconds, the aforementioned delay wires are made of regular passive wires, as can be found inside any digital circuit.

A first prototype has been implemented on an Altera Cyclone II field programmable gate array (FPGA) [2]. Such an FPGA is a digital device, which consists of a very large number of simple logical gates. These gates can be propperly interconnected by using a hardware description language. Because of this hardware-oriented realization approach, such a system can be operated *in situ*. Section 3 provides all the technical implementation details as well as the experimental setup. The practical experiments are summarized in Section 4, and show that already this first X-ORCA prototype yields a resolution of about 0.02 ns. Finally, Section 5 concludes this paper with a brief discussion.

2 The X-ORCA Localization System

This section presents the X-ORCA architecture in three parts. The first parts starts off by clarifying the physical setup and all the assumptions made in this paper. Then, the second part explains X-ORCA's core principles. In so doing, it makes a few assumptions that might *seem* practically implausible for some readers. However, the third part elaborates on how the X-ORCA architecture and the assumptions made in the second part can be fully realized on standard circuits.

2.1 Physical Setup and Preliminaries

Since the aim of a single X-ORCA instance is to determine the phase shift $\Delta\varphi$ between two incoming signals, it can be used as the core of a one-dimensional localization system. It thus adopts a standard setup (see, also, Fig. 1) in which a transmitter T emits a signal $s(t) = A\sin(2\pi f(t - t_0))$ with frequency f, amplitude A, and time offset t_0. Since this signal travels with the speed of light $c \approx 3 \cdot 10^8\,\text{m/s}$, it arrives at the receivers R_1 and R_2 after some delays $\Delta t_1 = (L + \Delta x)/c$ and $\Delta t_2 = (L - \Delta x)/c$.

Both receivers employ an amplifier and a Schmitt trigger, and thus feed the X-ORCA system with the two rectangular signals $r_1(t - t_0)$ and $r_2(t - t_0)$ that both heave frequency f. By estimating the phase shift $\Delta\varphi$ between these two signals $r_1(t - t_0)$ and $r_2(t - t_0)$, X-ORCA then determines the time difference $\Delta t = t_1 - t_2 = \Delta\varphi/(2\pi f)$, in order to arrive at the transmitter's off-center position $\Delta x = \Delta t c/2$.

It might be, though, that both the physical setup and the X-ORCA system have further internal delays, such as switches, cables of different lengths, repeaters, and further logical gates. However, these internal delays are all omitted, since they can be easily eliminated in a proper calibration process. Furthermore, for a real-world three-dimensional scenario, the X-ORCA system has to be simply duplicated twice.

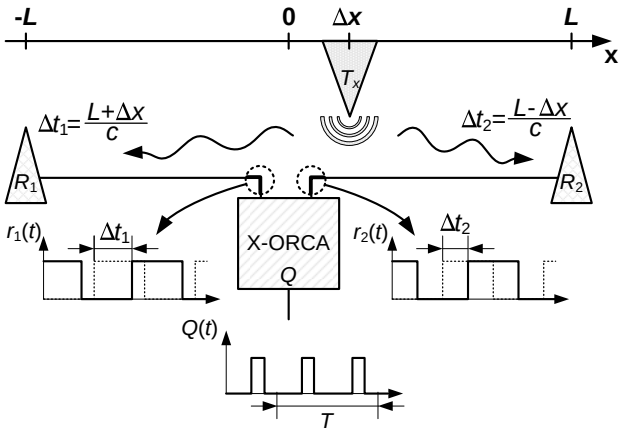

Fig. 1. X-ORCA assumes a standard, one-dimensional setup in which the time difference $\Delta t = t_1 - t_2 = 2\Delta x/c$ is a result of the transmitter's off-center position Δx. It indirectly determines $\Delta t = \Delta\varphi/(2\pi f)$ by estimating the phase shift $\Delta\varphi$ between the two incoming signals $r_1(t)$ and $r_2(t)$.

2.2 The System Core

Essentially, the X-ORCA core consists of a large number of independently operating phase detectors. One of these phase detectors is illustrated in Fig. 2. It consists of a logical XOR and a counter. The XOR "mixes" the two input signals s_1 and s_2, and yields a logical 1 or a logical 0 on whether the two signals

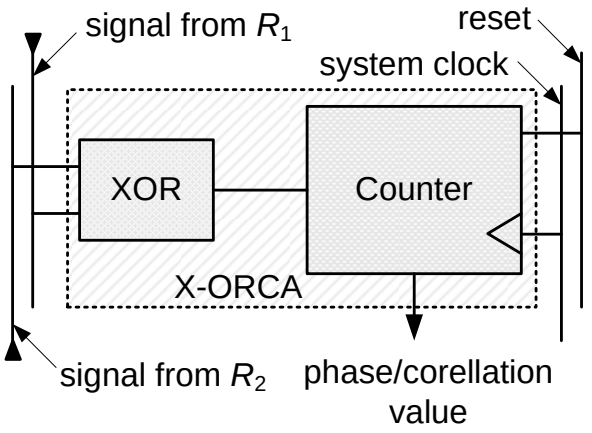

Fig. 2. An X-ORCA phase detector consists of a logical XOR (or any other suitable binary logic function), which "mixes" the two input signals s_1 and s_2, and an additional counter to actually determine the phase shift $\Delta\varphi$.

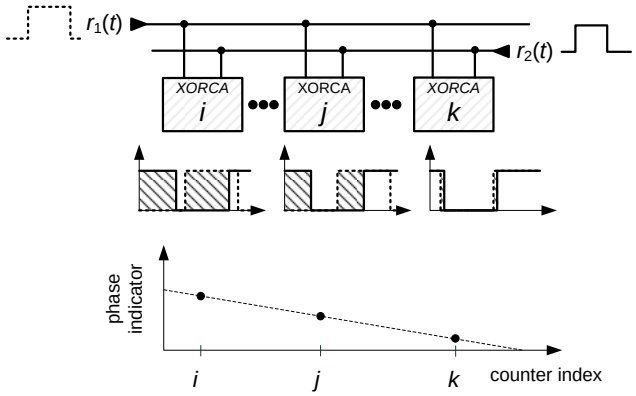

Fig. 3. X-ORCA places all phase detectors along two reciprocal (anti-parallel) "delay" wires w_1 and w_2 on which the two signals $r_1(t)$ and $r_2(t)$ travel with approximately two third of the speed of light $c_w \approx 2/3c$. Because the two wires w_1 and w_2 are *reciprocal*, all phase detectors have different internal delays τ_i.

differ or not. In other words, the degree of how both signals differ from each other corresponds to the phase shift $\Delta\varphi$, and is represented as the proportion of logical 1's per time unit. This proportion is evaluated by the counter that is attached to the XOR gate.

For example, let us assume an input signal with a frequency of $f = 100\,\mathrm{MHz}$ and a phase shift of $\Delta\varphi = \pi/4 = 45°$. Then, if the counter is clocked at a rate of 10 GHz over a signal's period $T = 1/(100\,\mathrm{MHz}) = 10\,\mathrm{ns}$, the counter will assume a value of $v = 25$.

At this point, three practical remarks should be made: (1) The XOR gate has been chosen for pure educational purposes; any other suitable binary logic function, such as AND, NAND, OR, and NOR, could have been chosen as well. (2) A counter clock rate of 10 GHz is quite unrealistic for technical reasons, but Subsection 2.3 shows how such clock rates can be virtually achieved. (3) A result of a phase shift $\Delta\varphi = \pi/4 = 45°$, for example, is intrinsically ambiguous, since the system cannot differ between $p = \pi/4 = 45°$ and $p = -\pi/4 = -45°$.

In order to solve the ambiguity of a single phase detector, X-ORCA simply employs more than just one. Figure 3 shows that X-ORCA places all phase detectors along two reciprocal (anti-parallel) "delay" wires w_1 and w_2 on which the two signals $r_1(t)$ and $r_2(t)$ travel with approximately two third of the speed of light $c_w \approx 2/3c$. Because the two wires w_1 and w_2 are *reciprocal*, all phase detectors have different internal delays τ_i which always add to the external delay $\Delta t = 2\Delta x/c$ that is due to the transmitter's off-center position Δx. As a consequence, each phase detector i observes an effective time delay $\Delta t + \tau_i$ and thus a phase shift $\Delta\varphi_i = 2\pi f(\Delta t + \tau_i)$.

Further post-processing stages become particularly easy, if the internal delays $\tau_i^{\max} - \tau_i^{\min} = T = 1/f$ span the entire range of a period T of the localization

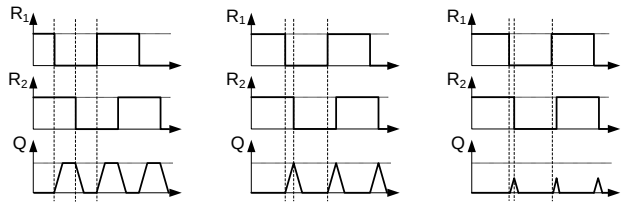

Fig. 4. Due to the inherent rise and fall times, a change in a gate's output requires some time. Therefore, if the input frequency increases too much or if the input edges come too close together, the gate cannot properly change its output (right-hand-side).

signal $s(t)$. For a first estimate of the transmitter's off-center position Δx it would suffice to determine the phase detector i that has the smallest counter value $v_i^{\min} = \min\{v_i\}$; only those phase detectors i have a counter value close to zero for which the condition $\tau_i \approx -\Delta T$ holds.

Furthermore, in case all phase detectors are sorted in an ascending order, i.e., $\tau_i \leq \tau_{i+1}$, the counter values v_i assume a V-shaped curve. Thus, X-ORCA might also be utilizing all phase detectors for reconstructing Δx by, for example, calculating the best-fitting-curve.

2.3 Real-World Implementation Details

The description presented in Subsection 2.2 has made a few, practically unrealistic assumptions, which are more or less concerned with the maximal frequency f that can be processed by the phase detectors. First of all, the X-ORCA concept has assumed that the clock frequency $\text{clk} \geq 100 \times f$ is at least 100 times higher than the frequency of the localization signal $s(t)$ in order to achieve a practically relevant resolution. A signal frequency of $f = 100\,\text{MHz}$, for example, would require a clock frequency of at least $\text{clk} = 10\,\text{GHz}$. Such a clock frequency, however, would be way too unrealistic for low-cost devices, such as FPGAs.

In case of periodic localization signals, however, a virtually very high frequency can be achieved by a technique, known as unfolding-in-time [6]. Let us assume, for example, a signal with frequency f and thus a period of $T = 1/f$. Then, the samples could be taken at $0, t, 2t, \ldots, (n-1)t$, with $t = T/n$ denoting the interval between two consecutive samples, and n denoting the number of samples per signal period T. Then, unfolding-in-time means that the samples are taken at $0, (t+T), 2(t+T), \ldots, (n-1)(t+T)$. That is, the sampling process is expanded over an extended interval with duration nT. Moreover, unfolding-in-time does not necessarily stick to an increment of "$t + T$". For example, the samples can also be taken at $0, (kt + T), 2(kt + T), \ldots, (n-1)(kt + T)$, with k denoting a constant that is prime to n.

The second assumption concerns the electrical transition behavior of the XOR gates as well as the counters. The conceptual description of Subsection 2.2 implicitly assumes that gates and counters are fast enough to properly process

signals that travel along the internal wires with about two third of the speed of light. The technical suitability of this approach might be surprising to some readers but has already been shown by previous research [8]. That research has also shown that due to technical reasons, such as thermal noise, the logic gates do not yield exact results but that they exhibit a rather random behavior if, for example, set and hold time requirements are not met. This random effect can be *statistically* compensated, for example, by a large number of processing elements, which is another reason for employing a *large* number of phase detectors in the X-ORCA architecture.

The third implementation remark concerns the processing speed of the gates and the input parts of the counters. Figure 4 shows that if the phase shift gets too small (or too close to 180°), the rise and fall times prevent the gate from properly switching its output state. This effects lead to small errors of the counter values, if the phase shift $\Delta\varphi$ is close to zero or 180°; as a result, the expected V-shaped curve of the counter values (subsection 2.2) might change to a U-shape.

3 Methods

The first X-ORCA prototype was implemented on an Altera Cyclone II FPGA [2]. This device offers 33,216 logic elements and can only be clocked at about 85 MHz. The chosen FPGA *development board* is a low-cost device that charges about 500 USD.

On the top-level view, the X-ORCA prototype consists of 140 phase detectors, a common data bus, a Nios II soft core processor [3], and a system PLL that runs at 85 MHz. The Nios II processor manages all the counters of the phase detectors, and reports the results via an interface to a PC.

Due to the limited laboratory equipment, the transmitter, its localization signal $s(t)$, the two receivers R_1 and R_2, and their distances to the transmitter are all *emulated* on the very same development board. The transmitter and its localization signal $s(t)$ is realized by means of a second PLL, which runs at 300 MHz, whereas the receivers and physical distances are realized by means of some active delay lines.

It should be noted, though, that X-ORCA's internal "delay wires" w_1 and w_2 are realized as pure passive internal wires, connecting the device's logic elements, as previously announced in Subsection 2.2. In a second experiment, the prototype utilized an external 19 MHz signal and emulated the transmitter-to-receiver distances by external line stretchers [1].

4 Results

Figures 5-8 summarize the experimental results that the first X-ORCA prototype has achieved under different configurations. Unless otherwise stated, the figures present the counter values v_i of $n = 140$ different phase detectors, which were clocked at a rate of 85 MHz.

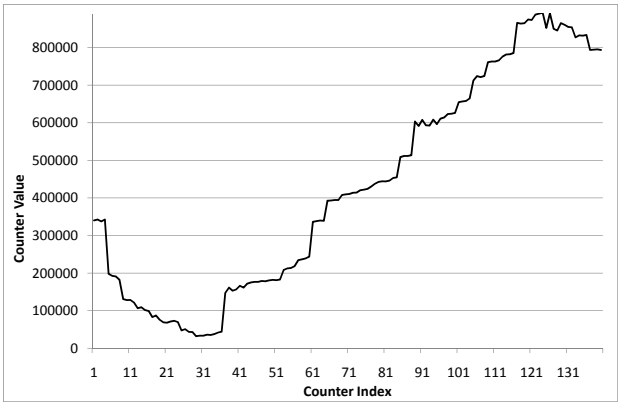

Fig. 5. The figure shows the counter values v_i of $n = 140$ phase detectors when fed with two 300 MHz signals with zero phase shift $\Delta\varphi = 0$.

In Fig. 5, the prototype was exposed to two 300 MHz (localization) signals that have a zero phase shift $\Delta\varphi = 0$. The input signals were sampled 1,000,000 times, which corresponds to an averaging over 196 periods, with virtually 5100 samples per period of the localization signal (please, see also the discussion presented in Subsection 2.3). It can be clearly seen that the minimum is at counter #31 and that the counters to the left and right have larger values as can be expected from X-ORCA's internal architecture. In addition, Fig. 5 reveals some technological FPGA internals that might be already known to the expert readers:

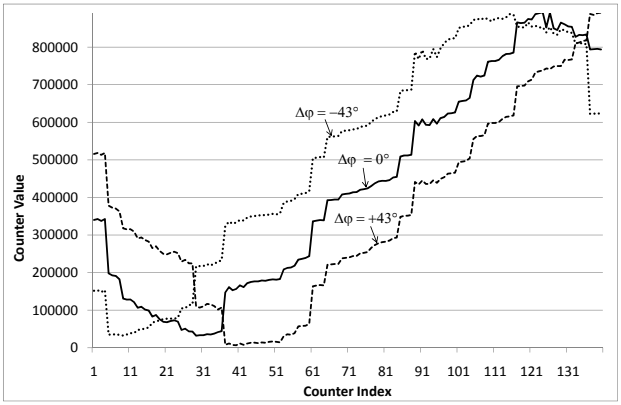

Fig. 6. The figure shows the counter values v_i of $n = 140$ phase detectors when fed with two 300 MHz signals with zero phase shift $\Delta\varphi = 0$ (solid line), with -43° phase shift $\Delta\varphi = -43^\circ$ (dotted line), and with $+43^\circ$ phase shift $\Delta\varphi = +43^\circ$ (dashed line).

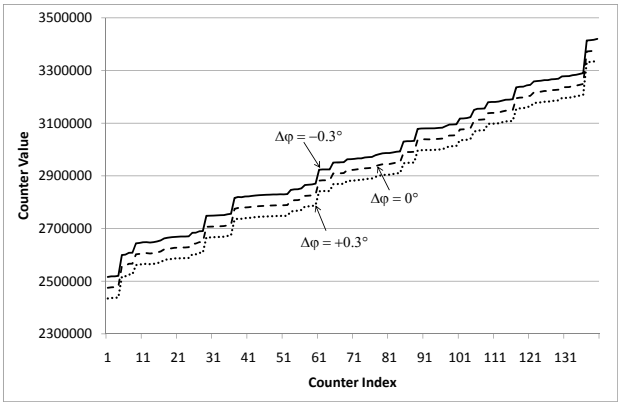

Fig. 7. The figure shows the counter values v_i of $n = 140$ phase detectors when fed with two 19 MHz signals with zero phase shift $\Delta\varphi = 0$ (dashed line), with about $-0.3°$ phase shift $\Delta\varphi \approx -0.3°$ (solid line), and with about $+0.3°$ phase shift $\Delta\varphi \approx +0.3°$ (dashed line).

neighboring logic elements do not necessarily have equivalent technical characteristics and are not interconnected by a regular wire grid. As a consequence, the counter values v_i and v_{i+1} of two neighboring phase detectors do not steadily increase or decrease, which makes the curve look a bit rough.

Figure 6 shows the results of the prototype when the two input signals have one of the following three time delays $\Delta t = t_1 - t_2 \in \{-0.4\,\text{ns}, 0\,\text{ns}, +0.4\,\text{ns}\}$. It can be clearly seen that a time delay of 0.4 ns shifts the "counter curve" by about 20 counters. This observation suggests that the prototype would be able to detect a time delay as small as $\Delta t = 0.02\,\text{ns}$.

A closer look at Figs. 5 and 6 reveals that the graphs are not exactly V-shaped but rather U-shaped at the very bottom. This is because the effects already discussed in Fig. 4 come into effect.

Figure 7 shows the behavior of the X-ORCA architecture when using the external 19 MHz localization signal. In this experiment, one of the connections from the function generator to the input pad of the development board was established by a line stretcher [1], whereas the other one was made of a regular copper wire. Figure 7 shows the values v_i of the $n = 140$ counters, which were still clocked at 85 MHz over a measurement period of 10,000,000 ticks. The three graphs refer to a phase shift of $\Delta\varphi \in \{-0.3°, 0°, +0.3°\}$, which corresponds to time delays $\Delta t \in -0.15\,ns, 0\,ns, +0.15\,ns$. It should be noted that the graph of this figure appears as a straight line, since the internal time delays τ_i span much less than an entire period of the 19 MHz signal, which is significantly lower than the previously used 300 MHz signal (both experiment have used exactly the same X-ORCA system).

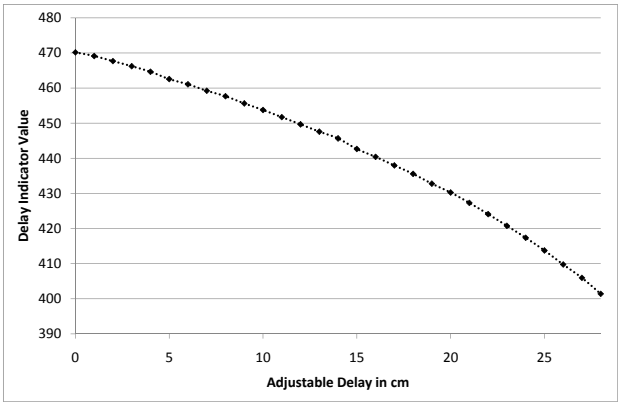

Fig. 8. The figure shows the delay value indicator resulting from adjustable delay line lengths when fed with two 19 MHz signals.

Figure 8 presents a different of Figure 7: In the graph, every dot represents the sum $v_{\text{tot}} = \sum_i v_i$ of all $n = 140$ counter values v_i; that is, an entire graph of Fig. 7 is collapsed into one single dot. The graph shows 29 measurements in which the line stretcher was extended by 1 cm step by step. It can be seen, that a length difference of $\Delta x = 1\,\text{cm}$ decreases v_{tot} by about 20. This result *suggests* that with a localization of 19 MHz, X-ORCA is able to detect a length difference of about $\Delta x = 1\,\text{mm}$, which equals a time resolution of about 0.015 ns.

5 Discussion

This paper has presented a new localization architecture, called X-ORCA. Its main purpose is the localization of transmitters, such as WLAN network cards or Bluetooth dongles, that emit electromagnetic signals. In its core, X-ORCA consists of a large number of very simple phase detectors, which are mounted along two passive wires with very small but finite internal time delays. This large number of rather unreliable phase detectors allows X-ORCA to perform a rather *reliable* statistical evaluation.

The X-ORCA architecture has been havily inspired by the biological role model, i.e., the auditory system of the barn owl. In this adaptation process, X-ORCA relys on a large number of rather unreliable simple phase detectors, which exhibit rather unreliable results. However, by averaging over a large number of entities, as the role model suggests, X-ORCA arrives at a quite reliable and accurate result.

Since the role model's neurons were emulated in re-configurable, physical hardware, the system is able to process electromagnetic signals, rather than acoustic signals. The switch in the utilized media is of practical importance for

many real-world applications, such as the localization of persons and/or objects in laboratory environments.

Unfortunately, the available laboratory equipment did not allow to test the true limits of the first prototype. This particularly applies to the maximal frequency f of the localization signal and to the achievable resolution with respect to Δx. These tests will be certainly subject of future research.

Future research will also be devoted to the integration of wireless communication modules. The best option seems to be the utilization of a software-defined radio module, such as the Universal Software Radio Peripheral 2 (USRP2) [5]. Finally, future research will port the first prototype onto more state-of-the-art development boards, such as an Altera Stratix V FPGA [4].

Acknowledgements

The authors gratefully thank Volker Kühn and Sebastian Vorköper for their helpful discussions. This work was supported in part by the DFG graduate school 1424. Special thanks are due to Matthias Hinkfoth for valuable comments on draft versions of the paper.

References

1. *Microlab: "Line Stretchers, SR series", Datasheed, Microlab Company*, 2008.
2. Altera Corp., San Jose, CA. *Nios Development Board Cyclone II Edition Reference Manual*, 2007. Altera Document MNLN051805-1.3.
3. Altera Corp., San Jose, CA. *Nios II Processor Reference Handbook*, 2007. Altera Document NII5V1-7.2.
4. Altera Corp., San Jose, CA. *Stratix V Device Handbook*, 2010. Altera Document SV5V1-1.0.
5. Ettus Research LLC. http://www.ettus.com.
6. J. Hertz, A. Krogh, and R. G. Palmer. *Introduction to the Theory of Neural Computation*. Addison-Wesley Pub. Co, Redwood City, California, 1991.
7. R. Kempter, W. Gerstner, and J. L. van Hemmen. Temporal coding in the submillisecond range: Model of barn owl auditory pathway. *Advances in Neural Information Processing Systems*, 8:124–130, 1996.
8. R. Salomon and R. Joost. Bounce: A new high-resolution time-interval measurement architecture. In *IEEE Embedded Systems Letters (ESL), Vol. 1, No. 2*, pages 56–59, 2009.